The Adhesion Strength of Twisted Glass Fiber Reinforced Epoxy Matrix Composites

Hashem M. HASSAN
University of Al-Qadisiya
Collage of Science

متانة التلاصق لليف زجاجي مفتول لتقوية شبكة الايبوكسي المتراكبة

هشام محمد علي حسن
كلية العلوم , جامعة القادسية

الخلاصة

أن من أهم العوامل المؤثرة على خواص المادة المتراكبة هي متانة التلاصق في المنطقة البينية بين الليف والمادة الحاضنة حيث تؤثر على اتجاه انتشار التشقق داخل المادة المتراكبة . الهدف من هذا البحث هو معرفة فيما إذا كان برم الليف له تأثير على متانة التلاصق في المنطقة البينية وذلك أولا بحساب إجهاد القص البيني باستخدام موديل كوكس (1) وثانيا حساب معدل الطاقة المتحررة باستخدام موديل نايرن (2,3,4) المتضمن تأثير الإجهاد الحراري و تأثير الاحتكاك , وقد تم استخدام النتائج العملية من فحص انسلاخ الليف (5) كقيم في كلا الموديلين . نتائج البحث أوجدت أن زيادة عدد اللفات لحزمة من ليف زجاجي ذات قطر (200 µm) يؤدي إلى زيادة إجهاد القص البني و معدل الطاقة المتحررة وذلك لزيادة طول المنطقة البينية التي يمر بها التشقق نتيجة حلزنة الليف, كما إن منطقة لاحتكاك في الرسم الباني للقوة– المسافة هي انزلاق خشن ويزداد بزيادة عدد اللفات.

Abstract

One of the important affects on the properties of composites is the adhesion strength at interface between the fiber and the matrix where could have a significant effect on crack propagation in the composites. The aim of this paper was to find that if the twisted bundle of glass fibers effected on the adhesion strength, i.e. the interfacial shear stress and the strain energy at interface of fiber reinforced polymer matrix composites, using, first, the interfacial shear stress by Cox model [1], second the energy release rate model derived by Nairn [2,3,4] which included the residual stress and friction effects as a theoretical analysis. The experimental part we used the microbond drag-out test [5] as tensile test. It was found when the turns numbers of glass fiber bundle of diameter (200 μm) about fiber axis increased the full debond force increased, so the interfacial shear stress and the energy release rate (strain energy) increased. Because the restrained of crack propagation increased as the screw thread pitch increased. The friction region in force-displacement curves for glass fiber bundle where the fiber twisted or not, was slip hardening and increased as twist number increased.

Introduction:

The engineering importance of a composite material is that two or more distinctly different materials combine together to form composite materials which possesses properties that are superior, or important in some other manner, to the properties of the individual components [6]. The strength of composites material at interface between the fiber and the matrix which characterized by the interfacial shear stress and the energy release rate, which plays an important role in the performance and behavior of fiber reinforced composite materials. Many tests used to measure the maximum pull-out force but the recent one is the drag-out test [5,7] which used in this paper to measure the maximum pull-out force for twisted bundle of glass fiber reinforce epoxy matrix and from the force-displacement curve in the experimental part, the interfacial shear stress (IFSS) in MPa and the energy release rate G_∞ in J/m^2 would be calculated.

The interfacial shear stress [1] defined as the maximum pull-out force (F_p) divided by the adhesion area of the fiber.

$$\tau_{ifss} = \frac{F_p}{2\pi r_f l_e} \qquad \text{---------- 1}$$

Where:

F_p the maximum pull-out force or the full debond force (N)

r_f the fiber radius

l_e embedded length

IFSS physically mean the average interfacial shear stress at time of failure [4]. It might be useful for qualitative work but has several limitations when one desired more rigorous interfacial characterization. To derived more fundamental results about interfacial properties is to use fracture mechanics by recording the load required for crack to growth or the critical energy release G_{ic} as a function of current crack length and other relevant specimen geometry which can effected by many factors such as embedded length , fiber and matrix materials , cure time and internal stress. In this paper the energy release rate using the same mathematical model of single fiber by Nairn including the effect of friction and internal stress [4,6] used to calculate the effect of twisting fiber (number of turns about its axis per embedded length) for U-shaped specimen.

2- The Energy Release Rate Model :

From the energy-based criteria [3,4,6,7,8] which depend on two concentric cylindrical model with a crack length (a) in a region at which the fiber enter the matrix fig (1)

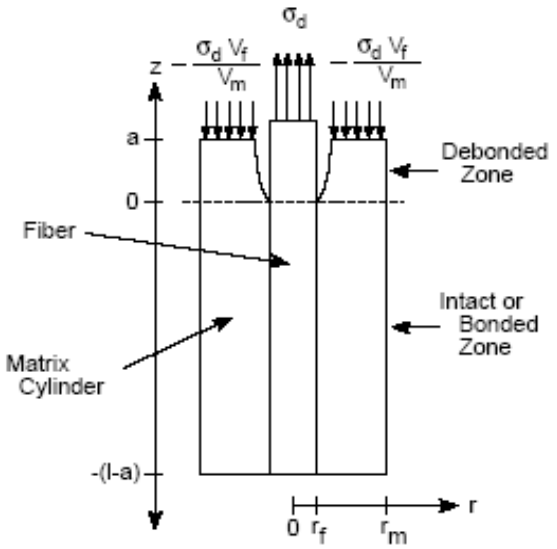

Fig (1) : The coordinate system used for the axisymmetric stress analysis of two concentric cylinders.
The origin of the *z* axis is placed at the debond tip. The zone $0 < z < a$ is the debonded zone. The zone $(l - a) < z < 0$ is the intact or bonded zone.

The energy release rate of crack length (a) written as:

$$G_{\infty}(a) = \frac{r_f}{2}(\sigma_d - ka)^2 + \frac{r_f}{2} D_{3s}(2 + C'_T(a))(\sigma_d - ka)\Delta T + \frac{r_f}{2}[(\frac{D_3^2}{C_{33}} + \frac{v_m(\alpha_T - \alpha_m)^2}{v_f A_o} + \frac{2D_3 D_{3s}}{C_{33}} C'_T(a))\Delta T^2 - kD_{3s}C_T(a)\Delta T]$$

---------- 2

$C_T(a)$ is the cumulative stress transfer function defined by

$$C_T(a) = \int_0^{l-a} F(z)dz \quad \text{---------- 3}$$

And

$$F(z) = \frac{\sinh\beta(l-a-z)}{\sinh\beta(l-a)} \quad \text{---------- 4}$$

β is the shear-lag parameter defined as [8,9,10] .

$$\beta^2 = \frac{2}{E_A E_m}\left[\frac{E_A v_f + E_m(1-v_f)}{\frac{1-v_f}{4G_A} + \frac{1}{2G_m}\left(\frac{1}{1-v_f}\left(\frac{1}{v_m}\ln\frac{1}{v_f} - \frac{3-v_f}{2}\right)\right)}\right] \quad \text{---------- 5}$$

All constants of equations (2) and (5) defined in the appendix, the term $(\sigma_d - ka)$ represent the difference between the stress applied to the fiber and the frictional stress transfer rate in the debonding zone multiplied by the crack length (a)

$$k = \frac{2T_f}{r_f} \quad \text{---------- 6}$$

In fig (2) F_{knik} is corresponding to zero initial crack length while F_p corresponding to the point at which the crack length is nearly equal to the length of droplet or l_e in equivalent cylindrical model, T_f is the absolute value of the constant interfacial friction stress which can determined form force-displacement curve after debonding (F_p) where:

$T_f = \frac{F_f}{2\pi r_f l_e}$, F_f is the friction force.

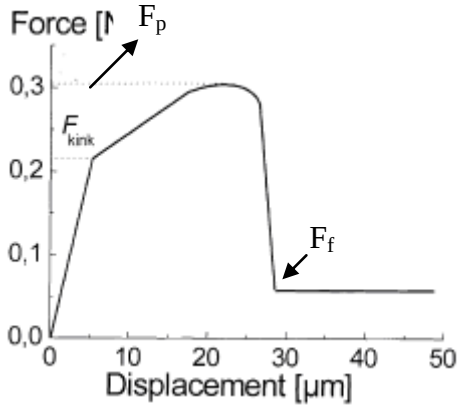

Fig (2): A typical force-displacement curve taken from pull-out test

Returning to equation (2) ΔT is the difference between the specimen temperature and the stress free temperature and with the thermal expansion coefficient equation (2) would include thermal stress addition to friction stress (k) and the external stress ($б_d$).
For a specimen without observed debond growth [5] and from force-displacement curve the peak debond force is corresponding to the point at which the debond reached the end of droplet then the critical energy release rate:

$$G_{ic} = \lim_{a \to l} G(a) \qquad \text{---------- 7}$$

To calculate G(a) in long –droplet limit or the limit as $l_e \to \infty$, the cumulative stress transfer function would be:

$$\lim_{l \to \infty} C'_T(a) = 0 \quad \text{and} \quad \lim_{l \to \infty} C_T(a) = \frac{1}{\beta}$$

The limiting energy release rate $G_\infty(a) = \lim_{l \to \infty} G(a)$

$$G_\infty(a) = \frac{r_f}{2}\left[C_{33s}(\sigma_d - ka)^2 + D_{3s}(2\sigma_d - k(2a + \frac{1}{\beta}))\Delta T + (\frac{D^2{}_3}{C_{33}} + \frac{v_m(\alpha_T - \alpha_m)^2}{v_f A_o})\Delta T^2 \right]$$

---------- 8

Where

$$\sigma_d = \frac{F_d}{\pi r_f{}^2}$$

The balance forces of a drag-out specimen shown in fig (3) if $l_1=l_2=l_{1/2}$ then the horizontal balance force f = 0 and the pull-out force $P_1=P_2=P$

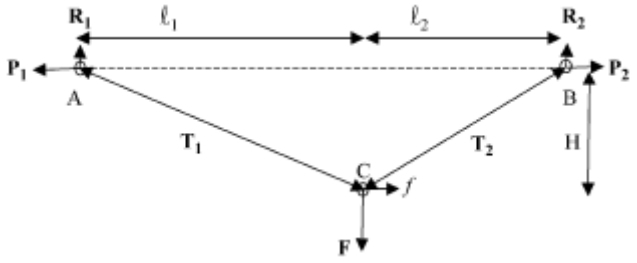

Fig (3): Force equilibrium for the drag-out configuration

To convert the drag-out force (F) to pull-out force (P) [3].

$$P = \frac{F}{2}\frac{l_{1/2}}{H} \qquad \text{---------- 9}$$

Where :
$l_{1/2}=l_1=l_2$ (when the balance force = 0)
H= cross head displacement
F= drag out force
P is the pull out force for one side of specimen

And to convert the drag-out cross-head displacement to pull-out displacement Δ:

$$\Delta = \sqrt{l_{1/2}^2 + H^2} - l_{1/2} \qquad \text{------- 10}$$

4- Sample Preparation:

A polysiloxane molds fig(4-a) cat by a razor, a bundle of E-glass fiber twisted with (0,5,7,10) turn s of the same radius (20011m) fixed at the razor cut fig(2-b), the fiber protrudes over few millimeter outside the specimen, similar to micobond test .these molds have different embedded lengths l, (2.6mm,3mm,3,4 mm,4mm,5mm,6 mm), then epoxy of three volume parts (hexandiodiglycidether resin and one part of 3,3 diaminodicyclohexyl-methane as hardener), the mixture purred slightly in U-shape polysiloxane mold with (5 mm) free fiber length and cured for five days at room temperature in order to minimize the internal stresses, epoxy-twisted glass fiber specimens fig (4-c) get out from the polysiloxane mold carefully after five days. The specimen attached to fixed grip of tensile tester (Instron 1122) and steel hook of diameter (2mm) fixed in the moving grip of the tensile tester used to drag the fiber fig (4-d).

Fig(4-a) : polysiloxane molds polysiloxane

Fig(4-b):Glass fiber fixed in mold.

Fig(4-c):Epoxy-glass fiber U-shaped specimen

Fig(4-d): U-shaped specimen under tensile tester

Fig(4) : The preparation of U-shaped specimen .

The test temperature ($\Delta T = -12C^0$) [11,12,13] and the force applied as well as the displacement recorded by Instron tester with drag-out rate 0.5 mm/min, the glass fiber and epoxy thermal and mechanical properties were same in references [2,4,6,8] .

4-Results and Discussion:

Figure (5) shows the relation between applied pullout force and the corresponding displacement of embedded fiber, the data of these curves taken from Instron recorder after used equations (6,7) (converting the drag-out force and displacement to pull-out force and displacement). In figure (5) the peak force due to crack length equal to the embedded length, the peak force (F_p) for each specimen tested recorded and then using equations (1,5,8,9) the results tabulated in tables (1,2,3,4). In these tables the energy release rate $G_\infty(l_e)$ J/m^2 as the embedded length increase would increased for all turn numbers because the interfacial area of twisted fiber increased. When the twisted bundle fiber dragging out, the crack propagated in smooth area at interface this because the glass fiber surface is more hardening than epoxy surface as in fig (5).

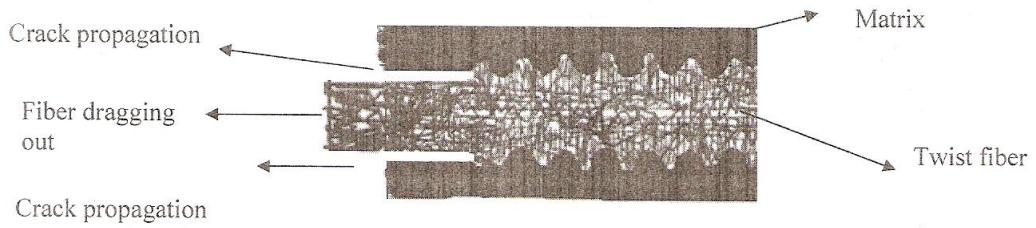

Fig (5): A schematic diagram represents the interface between the twist glass fiber and the epoxy matrix .

his could also seen in figure (6) at the friction part so the slip hardening [14] forced the friction region to be less than the peak force, for this reason the interfacial shear area taken to be ($2\pi r_f l_e$) which used in calculated the interfacial shear stress (equation (1)) and also when the energy release rate calculated (σ_d and T_f in equation (8)). From tables (1,2,3,4) and for same twist number there was no consistent relation found between the interfacial shear stress (IFSS) and embedded length or in other words the (IFSS) is not always increase as embedded length increase.

This due to the following two main causes:

1- Applied stress effected by residual thermal stress, this effect could be seen in the values of energy release rate with out thermal stress effect $G_\infty(l_e)$ at $\Delta T=0$ which is always less than the energy release rate $G_\infty(l_e)$.

2- During crack growth, the external load overcome not only forces of interfacial bonding in intact region fig (1), but also friction in already debonding region (friction region).This effect could be seen also in the values of $G_\infty(l_e)$ at k=0 .

The interfacial shear stress for embedded length (2.6mm) and for (zero turn, five turns, seven terns, ten turns) are respectively (15.3 MPa, 18.05 MPa, 31.26 MPa, 40.1 MPa) that is when the twist number increased the drag-out or pull-out force increased, which because of the restrained of crack propagation increased as the screw thread pitch increased.

In table (5) the results of testing the energy release rate for specimens of same embedded length and of different number of turns were tabulated .the energy release rate for embedded lengths (2.6mm,3mm,3.4mm,4mm, 4.6mm,5mm) increased as the number of turns (surface area) increased and this effect is specially obtained in long embedded length (5 mm).

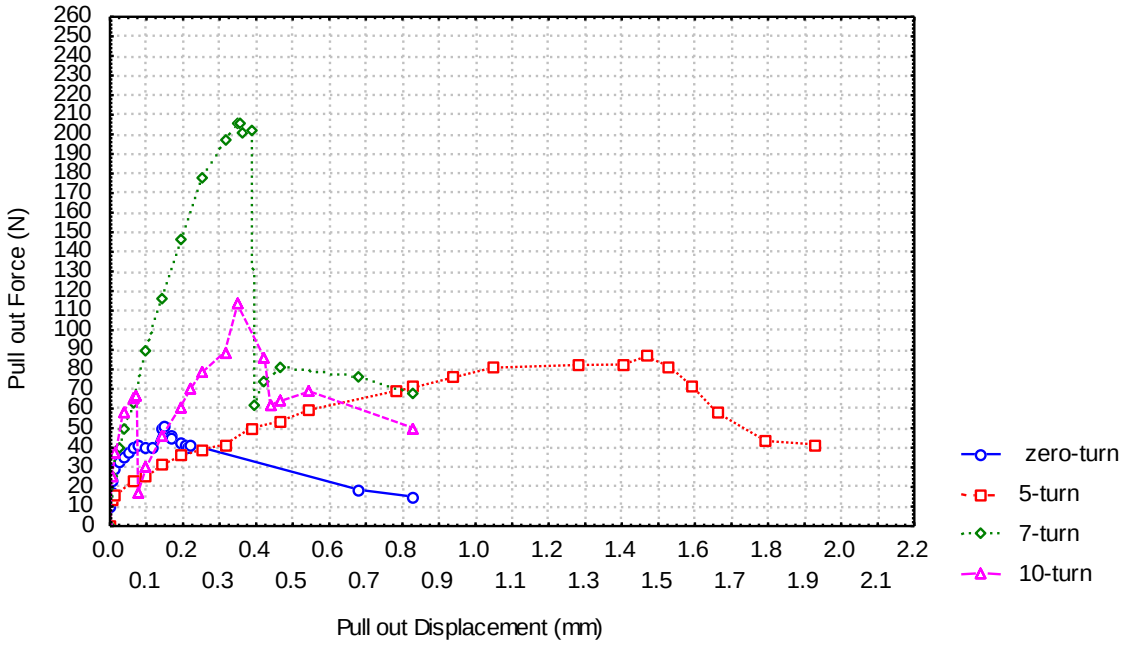

Fig (6): Pullout force vs. displacement of different twisted glass fiber reinforced epoxy matrix.

Table 1: Different embedded lengths of zero-turns
MATRIX-FIBER: Epoxy –glass fiber
Turn : zero -turn

Embedded length 4.0 mm (mm)	2.6 mm	3.0 mm	3.4 mm
Drag-out debond 85 Point (N)	24	205	267
Drag-out friction 35 Point (N)	20	215	100
Pull-out debond 119.38 Point (N)	50.4	235.1	94.7
Pull-out friction 64 Point (N)	6.5	184.06	44.4
IFSS at debond 23.74 Point (Mpa)	15.3	62.3	22.15
Shear-lag Parameter 1/β 1665.5 (μm)	1665.5	1665.5	1665.5
G∞(le) 154.3 J/m^2	103.8	116.26	129.34
G∞(le) at ΔT=0 135.9 J/m^2	85.07	115.2	112.06
G∞(le) at k=0 681.58 J/m^2	134.29	254.37	437.2

Table 2 : Different embedded lengths of 5-turns
MATRIX-FIBER: Epoxy –glass fiber
Turn : 5 -turn

Embedded length (mm)	2.6 mm	4.0 mm	4.0 mm
Drag-out debond Point (N)	60	52	142
Drag-out friction Point (N)	55	55	80
Pull-out debond Point (N)	59.05	82.2	83.58
Pull-out friction Point (N)	14	20.9	21.6
IFSS at debond Point (Mpa)	18.05	16.35	16.61
Shear-lag Parameter 1/β (μm)	1665.5	1665.5	1665.5
G∞(le) J/m^2	107.41	190.91	194.9
G∞(le) at ΔT=0 J/m^2	89.69	166.11	170.26
G∞(le) at k=0 J/m^2	179.49	334.6	334.9

Table 3 : Different embedded lengths of 7-turns
MATRIX-FIBER: Epoxy –glass fiber
Turn : 7 -turn

Embedded length (mm)	2.6 mm	3.4 mm	5 mm
Drag-out debond Point (N)	65	210	158
Drag-out friction Point (N)	84	180	82
Pull-out debond Point (N)	102.2	176.2	203.6
Pull-out friction Point (N)	44	100	120.01
IFSS at debond Point (Mpa)	31.26	41.24	32.39
Shear-lag Parameter 1/β (μm)	1665.5	1665.5	1665.5
G∞(le) J/m^2	169.23	280.2	336.7
G∞(le) at ΔT=0 J/m^2	150.03	257.8	309.57
G∞(le) at k=0 J/m^2	505.69	1450.2	1920.8

Table 4 Different embedded lengths of 10-turns:
MATRIX-FIBER: Epoxy –glass fiber
Turn : 10 -turn

Embedded length 5.0 mm (mm)	2.6 mm	3.0 mm	4.6 mm
Drag-out debond 86 Point (N)	86	102	170
Drag-out friction 60 Point (N)	88	20	120
Pull-out debond 173.5 Point (N)	131.1	125	247.1
Pull-out friction 50.6 Point (N)	55	42	175
IFSS at debond 29.19 Point (Mpa)	40.1	33.14	42.73
Shear-lag Parameter 1/β 1665.6 (μm)	1665.5	1665.5	1665.5
G∞(le) 717.12 J/m^2	281.6	335.5	486.3
G∞(le) at ΔT=0 669.03 J/m^2	256.5	305.14	454.5
G∞(le) at k=0 1405.68 1405.68 J/m^2	816.2	744.5	2807.09

Table 5 : The energy release rate (J/m^2) of embedded length at different turns.

Embedded length l_e (mm)	G∞ at zero-turn	G∞ at 5-turn	G∞ at 7-turn	G∞ at 10-turn
2.6 mm 281.6 J/m^2	103.8 J/m^2	107.4 J/m^2	169.23J/m^2	
3 mm- 3.4 mm 235.5 J/m^2	122.8 J/m^2	---------	280.2 J/m^2	
4 mm- 4.6 mm 486.3 J/m^2	154.3 J/m^2	192.9 J/m^2	-------	
5 mm 717.12 J/m^2	----------	-------	336.7 J/m^2	

Appendix [2,6]

The defined A_i, C_{ij} , and D_i required for the calculations described in this paper are listed below:

$$
\begin{aligned}
v_f A_0 &= \frac{v_m(1-\nu_T)}{E_T} + \frac{v_f(1-\nu_m)}{E_m} + \frac{1+\nu_m}{E_m} \\
A_3 &= -\left(\frac{\nu_A}{E_A} + \frac{v_f \nu_m}{v_m E_m}\right) \\
C_{33} &= \frac{1}{2}\left(\frac{1}{E_A} + \frac{v_f}{v_m E_m}\right) - \frac{v_m A_3^2}{v_f A_0} \\
C_{33s} &= \frac{1}{2}\left(\frac{1}{E_A} + \frac{v_f}{v_m E_m}\right) \\
D_3 &= -\frac{v_m A_3}{v_f A_0}\left[\alpha_T - \alpha_m\right] + \frac{1}{2}\left[\alpha_A - \alpha_m\right] \\
D_{3s} &= \frac{1}{2}\left(\alpha_A - \alpha_m\right)
\end{aligned}
$$

Here v_f and v_m are the volume fractions of fiber and matrix within the droplet. For the concentric cylinders in macroscopic specimens

$$v_f = \frac{r_f^2}{r_m^2} \qquad \text{and} \qquad v_m = \frac{r_m^2 - r_f^2}{r_m^2}$$

E_A and E_T are the axial and transverse moduli of the fiber ,V_A and V_T are the axial and transverse Poisson's ratios of the fiber, E_m is the modulus of the matrix, V_m in the Poisson's ratio of the matrix, α_A and α_T are the axial and transverse thermal expansion coefficients of the fiber, and αm is the thermal expansion coefficient of the matrix. The fiber is treated as transversely isotropic with the axial direction along the axis of the fiber. The results for isotropic fibers are easily generated be setting $E_A = E_T = E_f$, $V_A = V_T = V_f$,and $\alpha_A = \alpha_T = \alpha_f$ where subscript f indicates thermomechanical properties of an isotropic fiber. The matrix is here always considered to be isotropic.

4- References :

[1] Cox.H.L ,"The Elasticity and Strength of Paper and Other Fibrous Materials", British J. of Applied Physics ,3,No.1 ,72-79, (1952)

[2] J.A.Nairn," Analytical fracture mechanics analysis of the pull-out test including the effect of friction and thermal stress",Advance composit letters, vo 19,2000,no 6,373-383.

[3] D.A.mendels,"Analysis of single –fiber fragmentation test",NPL Report MATC(A) 17,July 2001.

[4] J.A.Nairn,C.H.Liu,D.A.Mendels,"Fracture mechanics of single fiber pull-out test and microbond test including the effect of friction and thermal stresses",soc.composite,9-12,2001.

[5] S.Nuriel,A.katz,H.D.Wagner,"Measuring fiber-matrix interfacial adhesion by mean of Drag-out micromechanical test", Composites J.part(A)(2005)33-37.

[6] C.H.Liu,J.Nairn,"Analytical and experimental methods for a fracture mechanics interpretation of the microbond test including the effects of friction and thermal stresses",J.of adhesion and adhesive ,19(1999),59-70.

[7] R.J.Scheer,J.A.Nairn, "Comparison of several fracture mechanics methods for measuring interfacial toughness with microbond test",J.Adhe.,1995,Vol 53, p 45-68

[8] B.W.Kim,J.A.Nairn, "Experimental verification of the effects of friction and residual stress on the analysis of interfacial debonding and toughness in single fiber composites" J. material science,Vol 37,2002,P 3965-3972.

[9] J.A.Nairn,"On the use of shear-lag methods for analysis of stress transfer in unidirectional composite ",J.mechanics of materials 26(1997),63-80.

[10] J.A.Nairn,H.D.Wagner,"A revised shear-lag analysis of an energy model for fiber-matrix debonding ",Advance composite Letters ,vol.5,No.5, 1996,p131-135

[11] J.A.Nairn, "Generalized shear-lag analysis including imperfect interface",Adv.comp.Letters,in press,2005.

[12] D.A.mendels, Y.leterrier,J.A.mason,"Physical agening of interfaces in polymer composite ",Merseburg,Germany,27/09-01/10/98.

[13] D.A.mendels, Y.leterrier,J.A.mason ,"Modeling of composite interfaces subjected to thermal stress and physical aging",99,bruels,In print.

[14] Victor . C.Li ,Cynthia Wa,Shuxain. W.,A suhiaa.O and Tadashi , " Interface Tailoring for Strain-Hardening Polyvinyl Alcohol-Engineered Cementations Composite" ACI Materials J. , ,PP463-472 , September-October 2002 .